ELSEVIER

Journal of Chromatography A, 785 (1997) 35–48

JOURNAL OF CHROMATOGRAPHY A

Comparison of enhanced-fluidity and elevated temperature mobile phases for high-performance size-exclusion chromatography

Huimin Yuan, Susan V. Olesik*

Department of Chemistry, The Ohio State University, 100W. 18th, Columbus, OH 43210, USA

Abstract

The use of enhanced-fluidity liquid mixtures of tetrahydrofuran (THF)–CO_2 as the mobile phases in the separation of styrene and polystyrene standards by size-exclusion chromatography (SEC) was compared to high temperature SEC. The phase diagram of a THF–CO_2 binary system was determined. Adding CO_2 to THF or increasing the mobile phase temperature produce similar results in the observed chromatography. The pressure drop across the column decreases, the optimal linear velocity shifts to a higher value, the chromatographic efficiency increases and the analysis time shortens for silica-based or polymer-based columns. The combination of both approaches provided the greatest improvement in chromatographic performance for CO_2 proportions of 0–30% and temperatures of 24–100°C. Molecular weight calibration curves indicated that the SEC mechanism was maintained for these conditions. However, non-size-exclusion interactions were detected when the proportion of CO_2 in the mobile phase was 50% mole fraction or more. Under those conditions, temperature elevation no longer enhanced the performance of the size-exclusion separation. Instead, increased adsorption of the polymer was observed due to significant loss of mobile phase solvent strength. However, by increasing the pressure of the mobile phase, the solvent strength could be restored. © 1997 Elsevier Science B.V.

Keywords: Enhanced-fluidity liquids; Mobile phase composition; Size-exclusion chromatography; High-temperature SEC

1. Introduction

High-performance liquid chromatography (HPLC) is widely used in the separation and analysis of non-volatile compounds; supercritical fluid chromatography (SFC) typically provides higher efficiency and lower analysis times than HPLC, but the range of applications of SFC is limited by the low polarity of fluids used in SFC. Supercritical fluids have diffusion coefficients that are at least an order of magnitude higher than liquids and have viscosities that approach those of gases. To improve the performance of HPLC (higher efficiency, resolution and speed of analysis), numerous attempts have been made to lower the mobile phase viscosity and increase the performance of the separation. In size-exclusion chromatography (SEC), selectivity cannot be changed significantly by mobile phase selection, because under ideal SEC conditions, the separation is based solely on the equilibrium distribution of the solute between the bulk solvent and the solvent occupying the pores. Therefore, viscosity reduction of the mobile phase appears to be particularly important for SEC.

Previous attempts to lower the mobile phase viscosity in SEC include the use of supercritical fluids as the mobile phase or increasing the mobile phase temperature. In order to minimize non-size-exclusion interactions, the Hildebrand solubility parameter of the mobile phase must be similar to that

*Corresponding author.

0021-9673/97/$17.00
PII S0021-9673(97)00573-6

of the stationary phase. Accordingly, in supercritical fluid SEC, the low densities of supercritical fluids restrict the selection of mobile phase solvent. Therefore, only solvents with high solubility parameters in the supercritical state were used; also, high pressures were employed to further enhance the solvent strength [1,2]. Other attempts to reduce the mobile phase viscosity in SEC involved limited temperature elevation [3–7]. In these studies, temperatures of up to 150°C were used. Significant gains in efficiency and speed of analysis were generally observed.

As an alternative means of reducing the mobile phase viscosity for SEC at room temperature, we previously investigated the use of enhanced-fluidity liquids [8], prepared by adding low viscosity liquid CO_2 to tetrahydrofuran (THF). Liquid CO_2 has a viscosity of 0.01 cP at 25°C, 170 atm [9], notably lower than that of THF, which is 0.35 cP at 20°C. Accordingly, the mixtures of THF–CO_2 have lower viscosities than THF. By using enhanced-fluidity liquid mixtures, the positive attributes of a supercritical fluid (fast mass transfer) is partially provided to HPLC at room temperature. Higher efficiency and shorter analysis times were achieved in the SEC separation of polystyrene standards by using THF–CO_2 mixtures [8]. The advantage of using enhanced-fluidity liquid mixtures, such as methanol–H_2O–CO_2 [10,11], methanol–CO_2 [9] and hexane–CO_2 [12] for reversed-phase-, porous glassy carbon- and normal phase HPLC separations were also characterized previously.

Temperature elevation and the use of enhanced-fluidity liquids decrease the viscosity of the solvent similarly; however, the scope of both methods is limited. The amount of added CO_2 is restricted by the solvent strength of THF–CO_2 mixtures. The applicability of the temperature elevation is restricted by the thermal stability of the analyte as well as by the thermal stability of the stationary phase. Therefore, the combination of using enhanced-fluidity liquid mobile phases and increasing temperature may be an alternative choice to provide further improvements in the performance of SEC.

In this study, both approaches to viscosity reduction in SEC are quantitatively compared for the separation of polystyrene standards. Emphasis was placed on characterizing the possible range and limitations of using the combination of THF–CO_2 and elevated temperature. Calibration curves were constructed for molecular weight determinations and for evaluation of the separation mechanism. The effects of temperature, CO_2 mole fraction and pressure on the separation were also illustrated by a series of chromatograms.

2. Experimental

2.1. Chromatographic system

The chromatographic system used in this study was previously described [8] with the exception that in this study an oven (Perkin-Elmer Corporation) was added to elevate the temperature of the column. The mobile phase was preheated for the elevated temperature studies by placing a 1-m length of stainless steel tubing inside the oven after the pump and before the injector, therefore, expansion of the mobile phase at the inlet of the column was minimized. Other chromatographic components include an ISCO 260D syringe pump (ISCO, Lincoln, NE, USA) for the solvent delivery system, a Valco W-series high pressure injection valve (Valco Instruments, Houston, TX, USA) with a 200-nl internal injection loop for sample injection and a Spectra 100 variable wavelength UV–visible absorbance detector (Thermo Separations, Fremont, CA, USA), equipped with a capillary flow cell. The detector excitation wavelength was 254 nm. A 30-μm I.D. fused-silica restrictor of an appropriate length was used to control the linear velocity of the mobile phase. A Setra model 204 pressure transducer (Setra Systems, Acton, MA, USA) was placed in-line after the detector and before the flow restrictor to monitor the pressure at the end of the column. Most of the data were obtained using a 250×4.6 mm I.D. Betasil silica column packed with 5 μm silica particles that had an average pore size of 200 Å (Keystone Scientific, Bellefonte, PA). For comparison of plate height data, separations using a polymer stationary phase (Jordi-Gel column, 100×4.6 mm I.D., packed with 5 μm divinylbenzene particles with small pores of ca. 300 Å from Jordi Associates, Bellingham, MA, USA) were also studied.

2.2. Phase diagram measurement system

The set-up for the phase diagram determination was described previously [13]. The main component was a high pressure, variable volume view cell (Temco, Tulsa, OK, USA) that can be operated up to 585 atm and a maximum temperature of ca. 180°C. The volume of the cell is changed by moving a displacer driven by a pneumatic assembly. The cell is also equipped with a stirring rod that can be moved back and forth from outside the cell through a magnetic coupling. The temperature of the cell contents was controlled by a CN9000 series temperature controller (Omega Engineering, Stanford, CT, USA) and measured to ±0.1°C by an Omegaclad type J thermocouple inside the cell. The pressure inside the cell was measured to ±0.4 atm by a Setra model 204 pressure transducer connected to the inside of the cell.

The following procedure was used to determine the phase transition point of each THF–CO_2 mixture. The view cell was first cleaned and flushed with CO_2 gas to remove any air from the cell. After the CO_2 used for leak checking was released, THF was delivered to the view cell with a 10 or 35 ml syringe. The quantity of THF delivered was determined by weighing the syringe before and after the delivery of THF to the view cell. Liquid CO_2 was transferred to the cell using a valved 40 ml stainless steel vessel (Whitey, Highland Heights, OH, USA), which was filled with CO_2 from a pump equilibrated at 122 atm. The amount of CO_2 delivered into the cell was controlled by monitoring the pressure increase inside the cell, while the exact quantity of CO_2 transferred into the cell was calculated using the weights of the vessel before and after the delivery. The CO_2 remaining in the cell after the initial flushing was also included in the calculation of the total amount of CO_2 delivered into the cell.

To reach thermal equilibrium, the cell remained at the temperature of interest for at least 30 min. The pressure in the view cell was increased to at least 7.0 atm higher than the approximate phase separation point by compressing the cell volume. The pressure inside the cell was then released at a rate of approximately 0.1 atm/s, while the cell's contents were mixed constantly. The phase boundary was determined by the emergence of the first gas bubble from the liquid, as observed through the transparent borosilicate glass window of the view cell [13–15].

2.3. Diffusion coefficient determination system

The system used to measure diffusion coefficients of styrene in the enhanced-fluidity liquid mixtures was the same as that of the chromatographic system, except that the analytical column was replaced with an open tubular fused-silica column with the dimensions 17.45 m×98 μm I.D., wound in 8.5 cm diameter coils. The aspect ratio (ratio of the coil diameter to the tube diameter) should be as large as possible to avoid secondary flow contributions that may cause incorrect measurements when a coiled tube is used to determine the diffusion coefficient [16]. The aspect ratio in this experiment was 867. Secondary flow does not contribute to the flow pattern under these experimental conditions [17]. The flow cell for detection was created by removing the polyimide coating from a 5-mm length of the 98 μm I.D. tube and then centering that section of the polyimide tube in the detector flow cell. The inlet pressure of the capillary tubing was maintained at 190.5 atm.

2.4. Materials

SFC grade CO_2 (Air Products, Allentown, PA, USA) and stabilized analytical reagent grade (99.9%) THF (Mallinckrodt, Paris, KY, USA) were used as received. The test solutes for chromatograms were polystyrene standards (M_w=382 100 with M_w/M_n=1.16, M_w=13 104 with M_w/M_n=1.04, M_w=2360 with M_w/M_n=1.08) and styrene, obtained from Aldrich (Milwaukee, WI, USA). For calibration curve construction, polystyrene standards of M_w=2 316 000, 114 200, 59 500, 18 700, 5120 with M_w/M_n=1.02, 1.04, 1.06, 1.03 and 1.08, respectively, were purchased from SP^2 Scientific Polymer Products, (Ontario, NY, USA), polystyrene (M_w=756 with M_w/M_n=1.08) and dibutylphthalate (99+%) were obtained from Aldrich. Di-*n*-hexylphthalate and di-*n*-decylphthalate were obtained from Chem Service (West Chester, PA, USA).

The test solutes were prepared as THF solutions with concentrations of 0.16–16 mg/ml each, for chromatograms. The concentration of styrene used

for the diffusion coefficient experiment was 0.11 mg/ml in THF. Using such a solution and a 200-nl injection loop, 0.02 μg of styrene were injected each time. The concentrations of dibutylphthalate and styrene used for the Jordi Gel column were 0.45 and 0.19 mg/ml, respectively.

The method used to prepare THF–CO_2 mixtures was described previously [8]. Basically, two syringe pumps were employed. First, a known amount of THF was filled into the empty pump, then a specific amount of pure CO_2 was transferred to it from the second pump that contained pure CO_2 and which was maintained at a constant pressure of 238 atm. The CO_2 volume needed to reach a specific mole ratio of THF–CO_2 in the pump was calculated based on CO_2 density at 238 atm and the temperature of the syringe pump. The THF–CO_2 mixtures were allowed to equilibrate for 12 h before use.

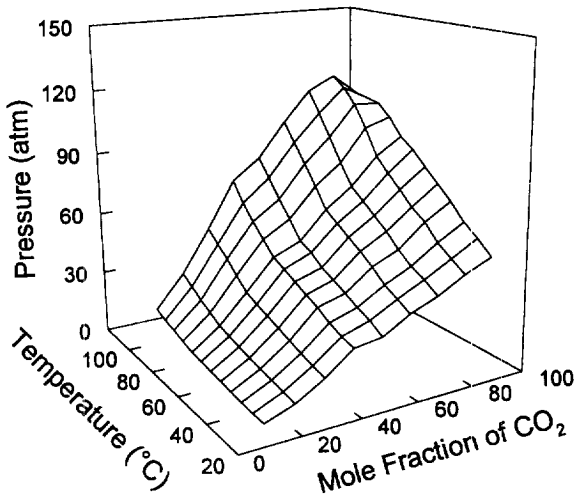

Fig. 1. Three dimensional phase diagram of a THF–CO_2 mixture.

2.5. Data analysis

The chromatographic data were collected using an EZChrom chromatography data system (Scientific Software, San Ramon, CA, USA) running on a pentium-based computer. Data were collected at different sampling rates that were controlled by the analysis time of the separation. Data were analyzed using Peakfit v. 4.0 for Windows (Jandel Scientific, San Rafael, CA, USA). Peak widths at half height were determined by fitting the chromatographic band to a Gaussian distribution.

3. Results and discussion

3.1. Phase diagram

The pressure throughout the chromatographic column should be maintained higher than the THF–CO_2 phase boundary to ensure single liquid phase mixtures of THF–CO_2. Nine THF–CO_2 mixture compositions were studied across the 10–90 mole% CO_2 range for temperatures ranging from 25–100°C. Fig. 1 shows a three dimensional phase diagram demonstrating the single phase region for THF–CO_2 mixtures with different temperatures. Each intersection in the grid surface represents one pressure–temperature-composition measurement and is an average of at least four determinations. The region above the meshed surface is a single phase of either liquid or supercritical fluid. While the region below the surface is a two-phase liquid–vapor region or a single phase vapor region when at very low pressures. Since we were interested in the location of the single phase region, efforts were not made to find the critical points of THF–CO_2 mixtures. Below the critical point, the phase transition point was observed when a bubble of vapor appeared at the top of the cell. Near and above the critical point, a fine mist (dew point) appeared in the cell. In the temperature range studied herein, only 20:80 and 10:90 mole fraction THF–CO_2 mixtures showed dew points at 70 and 55°C, respectively. If pressures >110 atm are used, single phase conditions are assured when temperatures are ≤100°C (see Fig. 1). Therefore, in this study, inlet pressures of 170 atm were used for Betasil silica columns and 190.5 atm for Jordi Gel columns.

3.2. Diffusion coefficients

To characterize the enhancement in mass transfer when CO_2 is added to THF and/or higher temperatures are used, diffusion coefficients of styrene were measured. The chromatographic band broadening method developed by Giddings and Seager [18] was used. Polymers were not used in this determination

to avoid the interference of their molecular weight distributions, which also broaden the chromatographic bands. Solute diffusion coefficients in other enhanced-fluidity mixtures [10], as well as binary and ternary supercritical fluid mixtures, were reported previously [19]. In this method, the analyte is introduced into a capillary tube as a short pulse and eluted as a Gaussian peak. The peak variance (σ^2) can be expressed as:

$$\sigma^2 = \frac{2D_{12}L}{u} + \frac{d^2uL}{96D_m} \quad (1)$$

where d and L are the diameter and length of the tubing, respectively; u is the average linear velocity and D_m is the diffusion coefficient of the solute. Eq. (1) is valid in an open tube if

$$\sigma < t, \quad Ld/tD_m > 100 \quad \text{and} \quad tD_m/d^2 > 0.2$$

where t is the elution time of the peak [20,21]. These requirements were satisfied by the experimental conditions used in this study. For Eq. (1), the first term ($2D_{12}L/u$) describes molecular diffusion along the axis of the column and is negligible if the average linear velocity is greater than $140D_m/d$ [22]. The linear velocity was calculated by using the elution time of styrene. A linear velocity of around 2.5 cm/s, which is $>>140D_m/d$ for styrene, was maintained by adjusting the restrictor length for different mobile phases. The measured chromatographic bands were fit to a Gaussian peak to obtain the peak variance. The binary diffusion coefficient of styrene in mixtures was then calculated using Eq. (1).

Fig. 2 shows the variation of the diffusion coefficient for styrene as a function of temperature for pure THF, 80:20 and 60:40 mole fraction of THF–CO_2 over a temperature range from 24 to 80°C. Diffusion coefficients of styrene increased steadily with temperature elevation, irrespective of the nature of the mobile phase. At each temperature, the mobile phase with the highest proportion of CO_2 exhibited the highest diffusion coefficient. The combination of adding CO_2 and increasing the temperature provided the largest increase in the diffusion coefficient, because both actions substantially lowered the viscosity of the mobile phase. Diffusion coefficients of styrene with 60:40 mole fraction THF–CO_2 at 80°C had the highest value in the tested range, which is ca. 2.5 times that in pure THF at room temperature. Also, the diffusion coefficient of styrene in a 60:40 THF–CO_2 mixture at room temperature is comparable to that in pure THF at ~50°C. No CO_2 proportion higher than 40% was employed, because non-size-exclusion interactions were previously noted [8] with mobile phases containing higher amounts of CO_2 at 170 atm and 25°C.

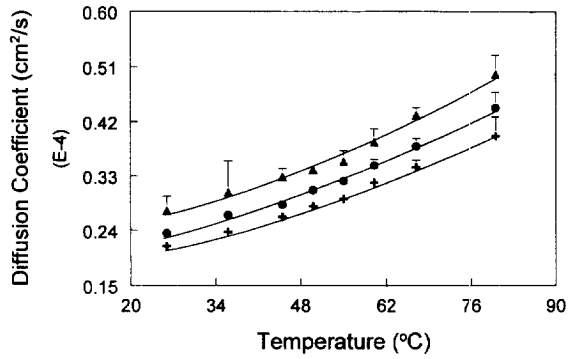

Fig. 2. Variation of the diffusion coefficients of styrene with different temperatures for different THF–CO_2 mixtures: (+) pure THF. (●) 80:20 THF–CO_2 (mole%), (▲) 60:40 THF–CO_2. Each data point is an average of four to six independent determinations.

3.3. Band dispersion curves and time of analysis

The chromatographic band dispersion in SEC can be described using Eq. (2) [23].

$$H_{TOT} = \left(A + \frac{\sigma^2_{dist}}{L}\right) + \frac{B}{u} + (C_f + C_{sm})u \quad (2)$$

The first term is a constant that includes the dispersion caused by multiple flow paths for the solute (A) and the inherent dispersion in the molecular weight distribution of the polymer. σ^2_{dist} is the standard deviation of the molecular weight distribution and L is the length of the column. B describes longitudinal diffusion (B) and is proportional to the diffusion coefficient of the analyte; C_f describes the contribution to band dispersion caused by the laminar flow profile in the tube and C_{sm} describes the dispersion in the "stationary" fluid within the pore structure.

The optimal linear velocity is determined by:

$$u_{opt} = \left(\frac{B}{C_f + C_{sm}} \right)^{1/2} \quad (3)$$

At linear velocities $> u_{opt}$, the plate height is predominantly controlled by the C_{sm} term, which is inversely proportional to the diffusion coefficient of the analyte, D_{12}. For a specific polymeric solute, the diffusion coefficient is proportional to the absolute temperature (T) and inversely proportional to the viscosity of the media (η) [24]:

$$D_{12} \propto \frac{T}{\eta} \quad (4)$$

Therefore, for a specific experimental condition, the plate height is mostly affected by the diffusion coefficient of the solute, which, in turn, is influenced by the temperature and the viscosity of the media. From Eq. (3), through the influence of the C terms, increasing temperature and/or lowering the viscosity by adding CO_2 results in a larger u_{opt}.

The reduced plate height versus linear velocity plots for styrene and polystyrene (PS) 13 104 are shown in Fig. 3A–B, respectively, for a constant inlet pressure of 170 atm, when pure THF and a 70:30 THF–CO_2 mixture and two temperatures, 24 and 80°C, were used with the Betasil silica column. These two solutes were selected to represent the behavior of totally penetrating and partially penetrating solutes. Linear velocities were calculated by using the retention time of a totally excluded polymer peak.

From the van Deemter curve for styrene (Fig. 3A), the shift of optimal linear velocity to a higher value with increasing temperature or the addition of CO_2 is clearly noted. It was not experimentally feasible to measure the u_{opt} for the polystyrene; the necessary linear velocities were too low. The slope of the H versus u curves at linear velocities $> u_{opt}$ also decreased for both PS 13 104 and styrene. Therefore, it is possible to choose a higher linear velocity without significantly affecting the plate height. This is advantageous when faster separations are required. The relative contribution of increasing temperature and adding CO_2 can also be evaluated. For styrene in Fig. 3A, increasing the temperature to 80°C with pure THF as the mobile phase produces an efficiency similar to that obtained by adding 30% CO_2 at 24°C.

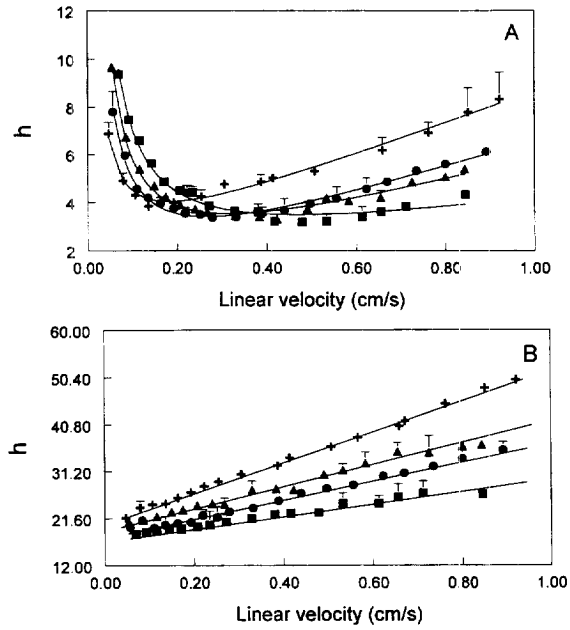

Fig. 3. Variation of reduced plate height of (A) styrene and (B) polystyrene 13 104 using a Betasil silica column with mobile phase linear velocity using different mobile phase compositions: (+) pure THF at 24°C, (●) 70:30 (mole%) THF–CO_2 at 24°C, (▲) pure THF at 80°C, (■) 70:30 THF–CO_2 at 80°C. Each value is an average of triplicate determinations. Error bars represent one standard deviation. For data points without error bars, the standard deviations are within the sizes of the data points.

Similar results were also observed for PS 13 104 (Fig. 3B).

To quantitatively examine the band dispersion, the H versus u curves for styrene were fit to the van Deemter equation, $H = A + B/u + Cu$, without the polydispersity term, by the non-linear least squares method with $r^2 \geq 0.98$ and those for PS 13 104 were fit to straight lines. The A, B and C constants for styrene and the slope for PS 13 104 are tabulated in Table 1 with their 95% confidence intervals. In addition to the four conditions used in Fig. 3, results from other conditions tested are also included in Table 1. For all of the conditions tested, A varied from $1.5 \cdot 10^{-4}$ to $7.6 \cdot 10^{-4}$, with no trends observed when the mobile phase conditions were changed. The B term, which describes longitudinal diffusion, increased with the temperature elevation and/or CO_2 addition. The C term decreased with temperature elevation and/or with CO_2 addition. The combina-

Table 1
Variation in van Deemter equation coefficients for styrene and the slope of Fig. 3B for polystyrene 13 104 as a function of mobile phase composition

Mobile phase composition	Styrene					PS 13 104 Slope $\times 10^{-3}$ [b] (s)
	$A\times10^{-4}$ (cm)	$B\times10^{-4}$ (cm^2/s)	$C\times10^{-4}$ (s)	$(B/C)^{1/2}$ (cm/s)	$H/u\times10^{-3}$ [a] (s)	
THF (24°C)	7.6±1.9[c]	1.2±0.2[c]	3.5±0.3[c]	0.183	9.0	15.7±0.5[c]
THF (80°C)	2.0±1.9	2.5±0.2	2.5±0.3	0.316	6.1	10.7±0.7
THF (100°C)	3.1±2.3	3.0±0.2	2.1±0.4	0.383	6.0	9.0±1.1
70:30 THF–CO_2 (24°C)	1.5±1.4	2.1±0.1	3.0±0.2	0.265	7.0	9.8±0.6
70:30 THF–CO_2 (60°C)	2.1±2.6	2.6±0.2	2.2±0.4	0.347	5.8	7.6±0.5
70:30 THF–CO_2 (80°C)	5.2±2.9	2.9±0.3	1.3±0.5	0.472	5.3	5.9±0.5
70:30 THF–CO_2 (100°C)	6.6±3.7	3.3±0.3	0.6±0.6	0.718	4.9	4.6±0.9

[a] H/u was calculated at a linear velocity of ~0.66 cm/s.
[b] Slopes of the fit line in Fig. 3B.
[c] 95% confidence intervals.

tion of CO_2 addition and temperature elevation gave the greatest decrease in the C term. Adding 30% CO_2 to pure THF decreased the C term to 86% of that at 24°C, while combining the use of 30% CO_2 with temperature elevation to 80°C lowered the C term further, to 37% of that at 24°C with pure THF. Higher temperatures clearly augment the effect of adding CO_2.

The $(B/u)^{1/2}$ values, which are proportional to u_{opt}, increased as the temperature increased and/or when more CO_2 was added (Table 1). For PS 13 104, the slope of the H versus u plot corresponds approximately to the C term at higher linear velocity. As expected, the change in slope for the polystyrene, with temperature elevation and CO_2 addition, was similar to the variation of the C term for styrene. For example, 70:30 THF–CO_2 at 100°C lowered the slope to 30% of that of pure THF at 24°C. The $H-u$ slopes for PS 13 104 were four–five times that of the C term of styrene under the same mobile phase conditions, indicating the smaller diffusion coefficient of the polymer compared with that of styrene.

The time of analysis of SEC is defined as the retention time for the totally penetrating analyte, which is the last eluted. The time of analysis, t, is directly related to the ratio of H/u [25].

$$t_r = \frac{16H}{S^2\left(\frac{\Delta M}{M}\right)^2 u}\left(1+\frac{K_{SEC}V_p}{V_0}\right) \quad (5)$$

where M is the molecular weight of the polymer, ΔM is the molecular weight interval that must be resolved at unit resolution, K_{SEC} is the distribution coefficient, V_p is the stationary phase volume or pore volume, S is the column's selectivity and the other variables were defined previously. The H/u values calculated at 0.66 cm/s for styrene and the slopes of the $H-u$ curve of PS 13 104 are also listed in Table 1. The H/u value for styrene decreased by approximately a factor of two on adding 30% CO_2 and increasing the temperature to 100°C, which should correspond to a similar decrease in the time of analysis.

Although silica-based packing materials provide better pressure and temperature stability, polymer gels are more commonly used for SEC of polymers soluble in organic solvents [26], partially due to the wider selection of pore sizes [27]. However, the chemical properties of these two packing materials are distinctly different. To investigate the effect of elevating temperature and using enhanced-fluidity liquid in polymer-based SEC, band dispersion curves were also constructed using a column packed with 100% polydivinylbenzene (Jordi Gel). Fig. 4A–B show the variation in band dispersion for styrene and dibutylphthalate (DBP), respectively, using the Jordi-Gel column. Four mobile phase–temperature combinations were chosen. These included pure THF and 60:40 mole% THF–CO_2 at 25 and 60°C. To minimize non-size-exclusion interactions when the 40% CO_2 mixture was used, a slightly higher pressure (190.5 atm) was used for these experiments

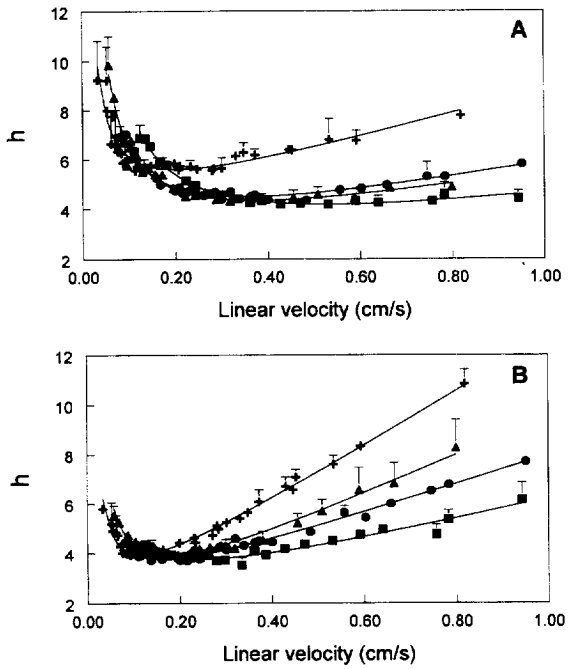

Fig. 4. Variation of reduced plate height of (A) styrene and (B) dibutylphthalate using a Jordi Gel polydivinylbenzene column with a mobile phase linear velocity using different mobile phase compositions: (+) pure THF at 24°C, (●) 60:40 (mole%) THF–CO_2 at 24°C, (▲) pure THF at 60°C, (■) 60:40 THF–CO_2 at 60°C. Each value is an average of triplicate determinations. Error bars signify standard deviations.

compared to that used for the silica-based column (170 atm). Similar gains in efficiency and speed of analysis were observed with the Jordi Gel column as with the silica-based column. Again, the combination of temperature elevation and CO_2 addition provided the greatest gain in both efficiencies and speed of analysis. The band dispersion curves for both styrene and DBP were refitted to the van Deemter equation without the polydispersity term; the *A*, *B* and *C* constants are summarized in Table 2. Analogous to the results with the Betasil silica column, the decrease in the *C* coefficient was similar when either the temperature was raised to 60°C or the proportion of added CO_2 was raised to 40%.

Although the mobile phase conditions employed were not exactly the same for the Betasil silica column and the Jordi Gel column, the observed variation in the constants (*A*, *B* and *C*) with temperature and CO_2 addition were similar (Tables 1 and 2). Both the *B*-term and the *C*-term are in the same range, respectively. For example, for the Betasil silica column, the *B*-term varies from $1.2 \cdot 10^{-4}$ to $3.3 \cdot 10^{-4}$ cm^2/s; and for the Jordi Gel column, it varies from $1.0 \cdot 10^{-4}$ to $3.1 \cdot 10^{-4}$ cm^2/s. The optimal velocities also resemble each other and are larger than that of DBP under similar conditions, reflecting the higher diffusion coefficient of styrene than DBP. The minimum plate heights of styrene

Table 2
Variation in van Deemter equation coefficients and their 95% confidence intervals for styrene and dibutylphthalate (DBP) using a Jordi Gel column

Mobile phase composition	Styrene			
	$A \times 10^{-3}$ (cm)	$B \times 10^{-4}$ (cm^2/s)	$C \times 10^{-3}$ (s)	$(B/C)^{1/2}$ (cm/s)
THF (25°C)	1.8±0.3	1.0±0.2	2.6±0.6	0.201
THF (60°C)	1.1±0.3	2.1±0.3	1.5±0.5	0.373
60:40 THF–CO_2 (25°C)	1.1±0.1	2.0±0.2	1.7±0.2	0.349
60:40 THF–CO_2 (60°C)	0.9±0.2	3.1±0.3	1.1±0.2	0.533
	DBP			
	$A \times 10^{-4}$ (cm)	$B \times 10^{-5}$ (cm^2/s)	$C \times 10^{-3}$ (s)	$(B/C)^{1/2}$ (cm/s)
THF (25°C)	6.7±1.2	7.6±0.8	5.7±0.3	0.116
THF (60°C)	5.2±1.9	12.5±1.6	4.2±0.3	0.173
60:40 THF–CO_2 (25°C)	8.8±1.4	8.7±1.6	3.0±0.2	0.169
60:40 THF–CO_2 (60°C)	8.1±2.7	13.5±4.0	2.2±0.4	0.249

achieved by both columns were similar (Figs. 3 and 4) with the Betasil silica column having slightly lower values of h_{min}. The only significant difference between the performance of the columns was that the Jordi-Gel column had a larger A-term than the Betasil silica column. The magnitude of the A-term provides information on the uniformity of the packed bed and has no bearing on the comparison made here.

3.4. Pressure drop

The pressure drop across the column is especially important for SEC, because increasing the column length or coupling multiple columns together is usually necessary, due to the low selectivity and low peak capacity of SEC. The pressure drop across a packed bed is directly related to the viscosity of the mobile phase as described by Darcy's law (Eq. (6)).

$$\Delta P = \frac{\phi \eta [u] L}{d_p^2} \tag{6}$$

ϕ is a dimensionless flow resistance parameter, η is the viscosity of the mobile phase, $[u]$ is average linear velocity, L is the column length and d_p is the particle diameter of the packing material. For a specific column, the slope of ΔP versus $[u]$ should be a constant that is related to the mobile phase viscosity if the stationary phase is rigid without change of d_p. Fig. 5 shows the pressure drop versus linear velocity for several mobile phase conditions used for the Betasil silica column. The data under each mobile phase condition were fit to straight lines with typical correlation coefficients of ≥ 0.90. The slopes decreased in the order of pure THF at 24°C, 70:30 THF–CO_2 at 24°C, THF at 80°C and 70:30 THF–CO_2 at 80°C. This implies that the viscosity is decreasing in that order. The slope for the second and third conditions are similar. The order of viscosity decrease for these two conditions is in accordance with that derived from the band dispersion curves of styrene. The effect of the combination of raising the temperature and using enhanced-fluidity liquids significantly exceeded that of employing them separately. For example, at a linear velocity of ~0.55 cm/s, an approximate 34 or 28% decrease in the pressure drop is observed when the temperature is increased to 80°C or 30% CO_2 is added to THF, respectively. Approximately a 50% decrease in the pressure drop is observed when 3% CO_2 is added to THF and the temperature is raised to 80°C.

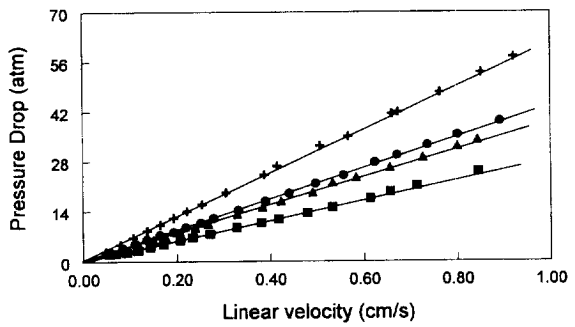

Fig. 5. Plot of the pressure drop across the Betasil silica column versus mobile phase linear velocity for different mobile phase compositions: (+) pure THF at 24°C, (●) 70:30 (mole fraction) THF–CO_2 at 24°C, (▲) pure THF at 80°C, (■) 70:30 THF–CO_2 at 80°C. An inlet pressure of 170 atm was maintained.

3.5. Molecular weight calibration curves

The molecular weight calibration curve of SEC is an important measure of the preservation of the size-exclusion separation mechanism. In this study, the molecular weight curves were constructed using thirteen different compounds, which covered analytes that totally penetrate the pore structure or are totally excluded. The calibration curves of the Betasil silica column for the four mobile phase–temperature conditions are shown in Fig. 6. The flow-rate was maintained at ca. 0.9 ml/min by adjusting the length of the restrictor. The retention volumes were calculated by multiplying the retention time by the flow-rate. Each point shown on the calibration curves was an average of two independent determinations. Compared to that obtained with pure THF at 24°C, using enhanced-fluidity liquid with 30% CO_2 and raising the temperature to 80°C or a combination of the two did not alter the global shape of the calibration curves significantly. Therefore, the solvent strength of the mobile phase was sufficient and the SEC mechanism was well maintained. Both curves constructed using mobile phases at 80°C were (pure THF or 70:30 THF–CO_2) shifted towards low retention volumes compared to those at

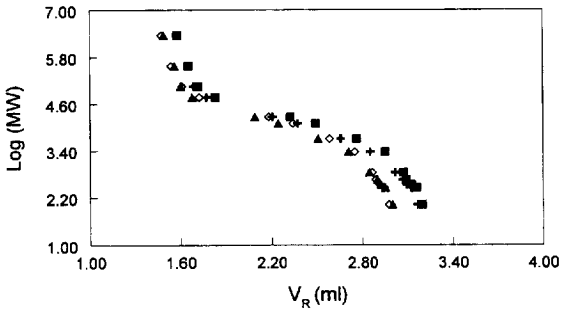

Fig. 6. Molecular weight calibration curves of the Betasil silica column using different mobile phase compositions: (+) pure THF at 24°C, (■) 70:30 (mole%) THF–CO_2 at 24°C, (▲) pure THF at 80°C, (◇) 70:30 THF–CO_2 at 80°C. A flow-rate of 0.90 ml/min was maintained by adjusting the length of the restrictor.

24°C. In fact, the decrease in retention volume with increased temperature is a phenomenon commonly observed irrespective of the mobile phase and the stationary phase used [5–7]. The proposed causes of this decreased retention include thermal expansion of the solute's hydrodynamic volume, swelling of gel to increase the internal volume and decrease the interstitial volume. The pore volumes calculated from the calibration curves for the four mobile phase conditions, THF at 24°C, 30% CO_2 at 24°C, THF at 80°C and 30% CO_2 at 80°C, are 1.59, 1.62, 1.51 and 1.50 ml, which constitute 38.4, 38.9, 36.3 and 36.1% of the total column volume, respectively. The small variation in the values indicates that the increased temperature and the addition of CO_2 affected the stationary phase minimally. However, within the small range of observed variation, the values are separated into two groups by the temperature. The higher temperature (80°C) gave a smaller apparent pore volume, while adding CO_2 exhibited no noticeable effect. Therefore, for molecular weight determinations, the addition of CO_2 may be preferable to temperature elevation.

3.6. Chromatograms

The separation of four analytes, three polystyrene standards and styrene, using the same inlet pressure and restrictor length (10 cm×30 μm I.D.) are shown in Fig. 7 for four different mobile phase conditions of THF and 70:30 THF–CO_2 at 24 and 80°C with the Betasil silica column. The retention times of

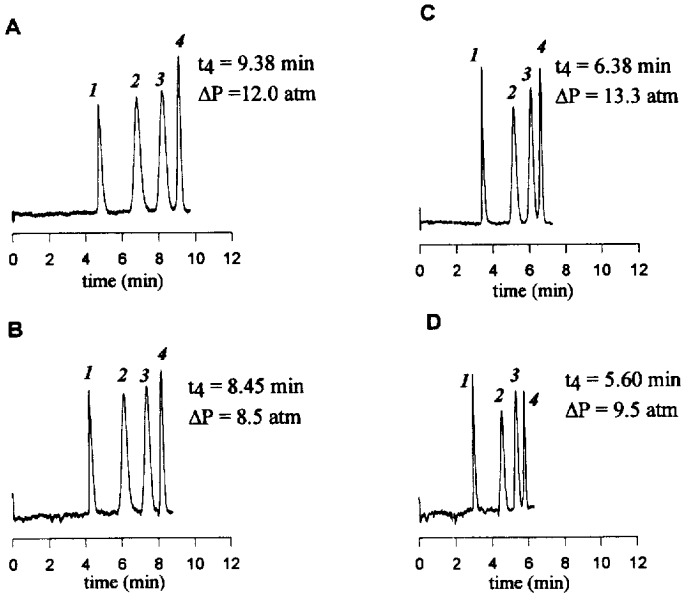

Fig. 7. Chromatograms of the separation of polystyrene standards 382 100, 13 104, 2360 (1 through 3, respectively) and styrene (4) using a Betasil silica column and four mobile phase compositions: (A) Pure THF at 24°C, (B) pure THF at 80°C, (C) 70:30 (mole%) THF–CO_2 at 24°C, (D) 70:30 THF–CO_2 at 80°C under the same restrictor (30 μm I.D. fused-silica) length of 10 cm. The retention times of styrene and the pressure drops were labeled for comparison.

styrene are shown in the chromatograms too. The retention times for each of the four analytes decrease in the order of THF at 24°C, THF at 80°C, 70:30 THF–CO_2 at 24 and at 80°C. Under the same conditions of inlet pressure and restrictor length, the decrease in retention time should be a reflection of the viscosity reduction in the mobile phase, which is the result of higher temperature, the addition of CO_2, or a combination of the two. If the retention time of styrene is taken as an example, compared to the condition of THF at 24°C, the elevation of column temperature to 80°C decreased the retention time by 10%, while the addition of 30% CO_2 decreased the retention time by 32%, and the combination of both achieved the highest effect, with the retention time lowered by 40%.

Chromatograms of the same mixture under conditions of constant flow-rate (0.9 ml/min) are shown in Fig. 8 for four mobile phase compositions: THF and 70:30 mole fraction of THF–CO_2 at 24 and 80°C with the Betasil silica column. Fig. 8D shows that the combination of the addition of 30% CO_2 and temperature elevation to 80°C increased the average plate numbers of the two polystyrene standards by ca. 160% and that of styrene by ca. 180%. Therefore, the use of enhanced-fluidity liquid at room temperature is a practical alternative for increasing the performance of SEC separation, which can be applied to temperature-sensitive analytes. When temperature elevation is also possible, the combination of an enhanced-fluidity mobile phase will substantially enhance the number of theoretical plates possible from a given column. Also, because the pressure drops across the column are lowered significantly, more columns can be connected in series to achieve an even greater number of theoretical plates.

While column efficiency provides a relatively indirect indication of the separation performance, resolution is a more direct assessment of the separation. The resolution of two adjacent peaks is defined as [28,29]:

$$R_s = \frac{\Delta V_r}{4\sigma} \tag{7}$$

where ΔV_r is the difference in the retention volume of the two peaks and σ is the average measured standard deviation of the retention volume. For SEC, the concept of specific resolution (R_{sp}) has been suggested to be a general measure of SEC resolution, and is expressed as a function of efficiency and selectivity [28,30]:

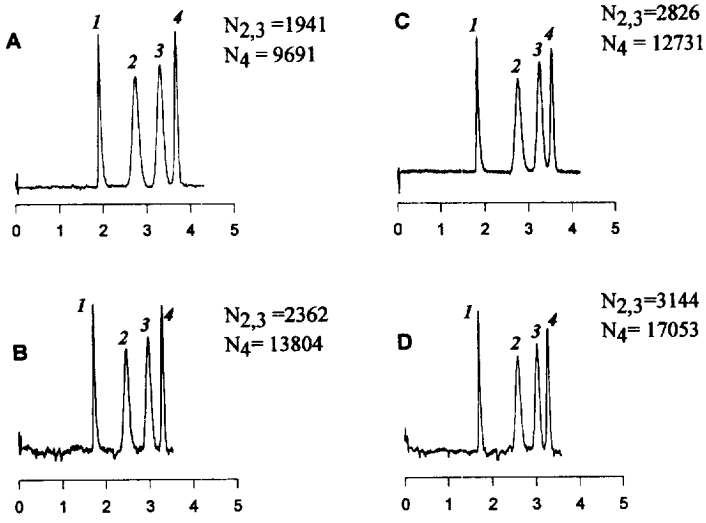

Fig. 8. Chromatograms of the separation of polystyrene standards 382 100, 13 104, 2360 (1 through 3, respectively) and styrene (4) with a Betasil silica column and the following mobile phase compositions: (A) Pure THF at 24°C, (B) pure THF at 80°C, (C) 70:30 (mole%) THF–CO_2 at 24°C, (D) 70:30 THF–CO_2 at 80°C. A flow-rate of 0.90 ml/min was maintained by adjusting the restrictor length. The average plate number of polystyrene standards 13 104 and 2360 and that of styrene are shown.

$$R_{sp} = \frac{0.58}{\sigma D_2} = \frac{0.58 \Delta V_r \sqrt{N}}{V_r \ln \frac{M_2}{M_1}} \quad (8)$$

where D_2 is the slope of the linear molecular weight calibration plot, M_1 and M_2 are the molecular weights of two narrow standards, N is the plate number of the peak and ΔV_r is the retention volume difference between two peaks. Therefore, SEC resolution is not only influenced by the efficiency, but is also affected by the slope of the calibration curve.

Table 3 lists the R_{sp} values of PS 13 104 and 2360 calculated using Eq. (8) for the four chromatographic separations in Fig. 8. The variation of specific resolution with the mobile phase condition showed similar trends to that found in efficiency. Either adding liquid CO_2 or increasing the temperature gave higher resolution. However, elevating the temperature appeared to cause a greater improvement on the resolution than adding CO_2. For instance, for PS 2360, compared to the R_{sp} using pure THF mobile phase at 24°C, the resolution using THF at 80°C and that using 30% CO_2–70% THF as the mobile phase at 24°C were higher. Similar trends were observed for PS 13 104. Nevertheless, for both solutes, the combination of adding CO_2 and elevating the temperature gave rise to the highest enhancement in resolution.

3.7. Effect of temperature elevation and pressure on enhanced-fluidity liquids in SEC

The results of previous sections showed that raising the temperature augments the effect of an enhanced-fluidity liquid mobile phase on optimal velocity, analysis time, pressure drop, plate height and resolution. The positive effects of temperature elevation up to 100°C were shown for enhanced-fluidity liquid with a CO_2 mole fraction up to 30% in THF, without exhibiting significant deviations from the ideal SEC mechanism at tested inlet pressures.

However, temperature elevation to further improve the performance of the THF–CO_2 mixture as the mobile phase is not without limitations. Raising the temperature causes thermal expansion of the solvent and reduces the density and solvent strength of the mobile phase at a constant pressure. Fig. 9 shows four chromatograms of separations on the Betasil silica column using a 50:50 THF–CO_2 mobile phase and four temperatures, i.e. 24, 60, 80 and 100°C, with a constant flow-rate of 0.9 ml/min. When 50% CO_2 was used at room temperature (Fig. 9A), the retention times of PS 13 104 and 2360 increased and the resolution between these peaks and styrene degraded. The peak height of the largest solute PS 382 100 sharply decreased and severe tailing of the peak was also observed. Increasing the temperature

Table 3
Variation in the specific resolution of polystyrenes 2360 and 13 104 with mobile phase composition at a constant flow-rate of 0.9 ml/min

Mobile phase composition	R_{sp}	
	PS 2360	PS 13 104
THF (24°C)	2.82±0.08	2.6±0.1
THF (80°C)	3.19±0.06	2.8±0.1
70:30 THF–CO_2 (24°C)	3.09±0.05	2.63±0.06
70:30 THF–CO_2 (80°C)	3.21±0.08	2.85±0.05

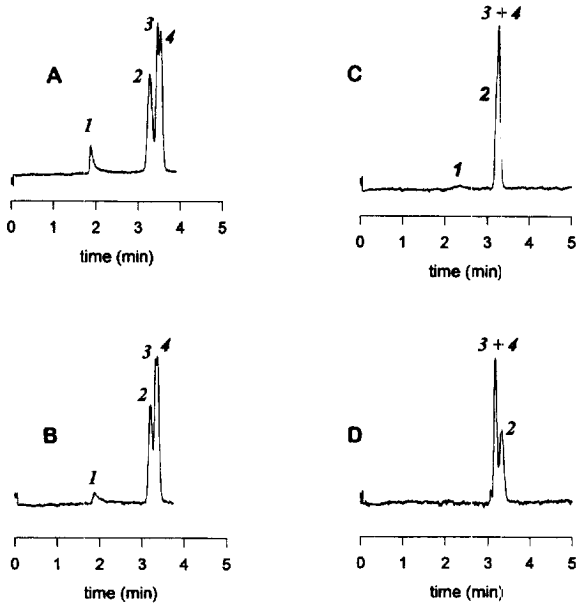

Fig. 9. Chromatograms of the separation of polystyrene standards 382 100, 13 104, 2360 (1 through 3, respectively) and styrene (4) by the Betasil silica column using a 50:50 (mole%) THF–CO_2 mobile phase with different temperatures: (A) 24°C, (B) 60°C, (C) 80°C and (D) 100°C. A flow-rate of 0.90 ml/min was maintained by adjusting the restrictor length. In (D), the peak for (1) polystyrene standard 382 100 did not elute.

to 60°C resulted in further deterioration. The peak height of PS 382 100 kept decreasing and tailing, a characteristic indication of adsorption. Upon increasing the temperature to 80°C, the peak of PS 382 100 almost disappeared, while the peaks of PS 13 104 and PS 2360 almost overlapped with that of styrene. At 100°C, the solvent strength decreased so much that PS 382 100 was totally adsorbed onto the stationary phase, while the further lag in the retention time of PS 13 104 reversed the SEC elution order with respect to PS 2360 and styrene.

Increasing the pressure, in contrast to raising the temperature, compresses the solvent and results in higher density and solvent strength at the same temperature. For example, under normal SEC conditions (i.e. solvent strength is high enough to minimize solute–gel interactions) with a Jordi Gel column using 60:40 THF–CO_2 at room temperature, minimal variation in the SEC performance occurred when the pressure was varied from 190.5 to 272 atm [31]. However, when the solvent strength of the mobile phase drops to where resolution is diminished or adsorption of solute to the stationary phase is observed, increasing the pressure can be of use in restoring the solvent strength of the mobile phase to a certain degree. For instance, in Fig. 9A, when a 50:50 mole fraction of THF–CO_2 mobile phase was used at 170 atm and 24°C on the Betasil silica column, the separation of the mixture showed a loss of resolution among PS 13 104 and styrene and severe tailing of PS 382 100. Fig. 10 (separation by the same Betasil silica column) compared to Fig. 9A shows that when the pressure was increased to 272 and 408 atm, the resolution among the last three peaks improved stepwise with the pressure increase, and the peak height and peak symmetry of PS 382 100 were also gradually restored. The peaks of PS 13 104 and 2360 were separated to almost baseline resolution at 408 atm, and the tailing of PS 382 100 was also notably improved.

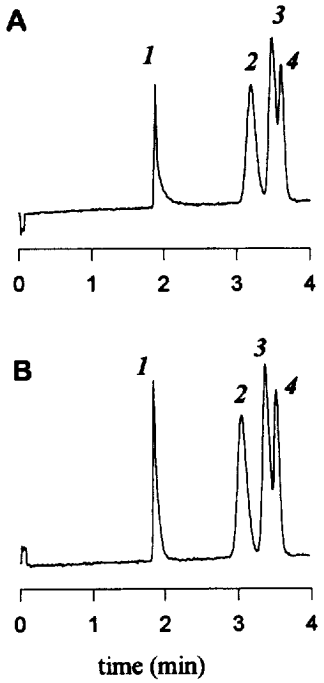

Fig. 10. Chromatograms of the separation of polystyrene standards 382 100, 13 104, 2360 (1 through 3, respectively) and styrene (4) by the Betasil silica column using a 50:50 (mole fraction) THF–CO_2 mobile phase with different pressures: (A) 272 atm and (B) 408 atm.

4. Conclusions

The enhanced-fluidity liquids lower the viscosity of the mobile phases, which provides similar advantages to SEC separations as observed with temperature elevation. These advantages include lower pressure drops, larger optimal linear velocity, higher efficiency and shorter analysis times. The addition of CO_2, like the elevation of temperature, slowly lowers the solvent strength. There are limitations to how much CO_2 can be added before the solvent strength is lowered too much and the retention mechanism changes. Similar problems result when too high a temperature is used.

For polymers that are thermally labile, the use of enhanced-fluidity liquids is preferred over temperature elevation. However, for thermally stable polymers, the combination of temperature elevation and the use of enhanced-fluidity liquids provide the largest gains in chromatographic performance.

Acknowledgements

The authors thank Keystone Scientific for supplying the columns for this study. We gratefully

acknowledge the support for this work by the National Science Foundation under Grant CHE-9503284.

References

[1] J.C. Giddings, L.M. Bowman, M.N. Myers, Anal. Chem. 49 (1977) 243.
[2] C. Fujimoto, T. Watanabe, K. Jinno, J. Chromatogr. Sci. 27 (1989) 325.
[3] C.N. Renn, R.E. Synovec, Anal. Chem. 64 (1992) 479.
[4] T. Takeuchi, S. Matsuno, D. Ishii, J. Liq. Chromatogr. 12 (1989) 987.
[5] S.R. Holding, G. Vlachogiannis, P.E. Barker, J. Chromatogr. 261 (1983) 33.
[6] S. Mori, T. Suzuki, Anal. Chem. 52 (1980) 1625.
[7] K. Unger, R. Kern, J. Chromatogr. 122 (1976) 345.
[8] H. Yuan, I. Souvignet and S.V. Olesik, J. Chromatogr. Sci., 35 (1997) in press.
[9] Y. Cui, S.V. Olesik, Anal. Chem. 63 (1991) 1812.
[10] S.T. Lee, S.V. Olesik, Anal. Chem. 66 (1994) 4498.
[11] Y. Cui, S.V. Olesik, J. Chromatogr. A 691 (1995) 151.
[12] S.T. Lee, S.V. Olesik, J. Chromatogr. A 707 (1995) 217.
[13] T.S. Reighard, S.T. Lee, S.V. Olesik, Fluid Phase Equilibria 123 (1996) 215.
[14] S.T. Lee, T.S. Reighard, S.V. Olesik, Fluid Phase Equilibria 122 (1996) 223.
[15] H.-S. Byun, B.M. Hasch, M.A. McHugh, Fluid Phase Equilibria 115 (1996) 179.
[16] R. Tijssen, Sep. Sci. Technol. 13 (1978) 681.
[17] R. Tijssen, Anal. Chim. Acta 114 (1980) 71.
[18] J.C. Giddings, S.L. Seager, J. Chem. Phys. 33 (1960) 1579.
[19] J.L. Woodruff, S.V. Olesik, Anal. Chem. 63 (1991) 670.
[20] V. Ananthakrishnan, W.N. Gill, A.J. Barduhn, AIChE J. 11 (1965) 1063.
[21] E. Grushka, E.J. Kikta Jr., J. Phys. Chem. 78 (1974) 2297.
[22] P.R. Sassiat, P.M. Mourier, M.H. Caude, R.H. Rosset, Anal. Chem. 59 (1987) 1164.
[23] J.V. Dawkins, G. Yeadon, J. Chromatogr. 188 (1980) 333.
[24] A. Rudin, H.K. Johnston, J. Polym. Sci. Part B 9 (1971) 55.
[25] J.C. Giddings (Editor), Advances in Chromatography, Vol. 20, Marcel Dekker, New York, 1982.
[26] H.G. Barth, B.E. Boyes, C. Jackson, Anal. Chem. 66 (1994) 595R.
[27] C. Wu (Editor), Handbook of Size Exclusion Chromatography, Marcel Dekker, New York, 1995, pp. 47–102.
[28] W.W. Yau and J.J. Kirkland, Modern Size-Exclusion Liquid Chromatography, Wiley, New York, 1975.
[29] J.J. Gunderson, J.C. Giddings, Anal. Chim. Acta 189 (1986) 1.
[30] J.J. Kirkland, Anal Chem. 64 (1992) 1239.
[31] H. Yuan, Ph.D. Dissertation, The Ohio State Univ., Columbus, OH, 1997.